

Supporting Information

Heteroepitaxial growth of highly anisotropic Sb₂Se₃ films on GaAs

Kelly Xiao¹, Virat Tara², Pooja D. Reddy¹, Jarod E. Meyer¹, Alec M. Skipper³, Rui Chen²,
Leland J. Nordin^{4,5}, Arka Majumdar^{2,6}, and Kunal Mukherjee^{1*}

¹ Department of Materials Science and Engineering, Stanford University, Stanford, CA 94305, USA

² Department of Electrical and Computer Engineering, University of Washington, Seattle, WA 98195, USA

³ Institute for Energy Efficiency, University of California Santa Barbara, Santa Barbara, CA 93106, USA

⁴ Department of Materials Science and Engineering, University of Central Florida, Orlando, FL 32816, USA

⁵ CREOL, The College of Optics and Photonics, University of Central Florida, Orlando, FL 32816, USA

⁶ Department of Physics, University of Washington, Seattle, WA 98195, USA

*Corresponding Author: kunalm@stanford.edu

A. Film Growth Parameters

Growth details for the films described in the main text are provided below in Table SI.

Table SI. Summary of growth parameters for Sb_2Se_3 thin films, including growth temperature (T_g), reconstruction symmetry, Sb and Se beam equivalent pressure (BEP), growth rate, and thicknesses. Thicknesses denoted with an asterisk are estimated values based on calculated growth rates.

T_g ($^{\circ}\text{C}$)	Reconstruction	Sb BEP (Torr)	Se BEP (Torr)	Growth Rate ($\text{\AA}/\text{s}$)	Thickness (nm)
265	Se-treated (2x1)	5.0×10^{-8}	1.0×10^{-6}	--	--
265	(2x1)	5.0×10^{-8}	1.0×10^{-6}	0.40	72
245	(2x1)	5.0×10^{-8}	1.0×10^{-6}	0.42	76
230	(2x1)	5.0×10^{-8}	1.0×10^{-6}	0.43	77
200	(2x1)	5.0×10^{-8}	1.0×10^{-6}	0.42	76
200	(2x1)	5.0×10^{-8}	1.0×10^{-6}	--	228*
180	(2x1)	5.0×10^{-8}	1.0×10^{-6}	--	--
150	(2x1)	5.0×10^{-8}	1.0×10^{-6}	0.44	79
<150	(2x1)	5.0×10^{-8}	1.0×10^{-6}	0.49	89

B. Disordered Phase Formation at Growth Temperatures of 150 $^{\circ}\text{C}$ and Below

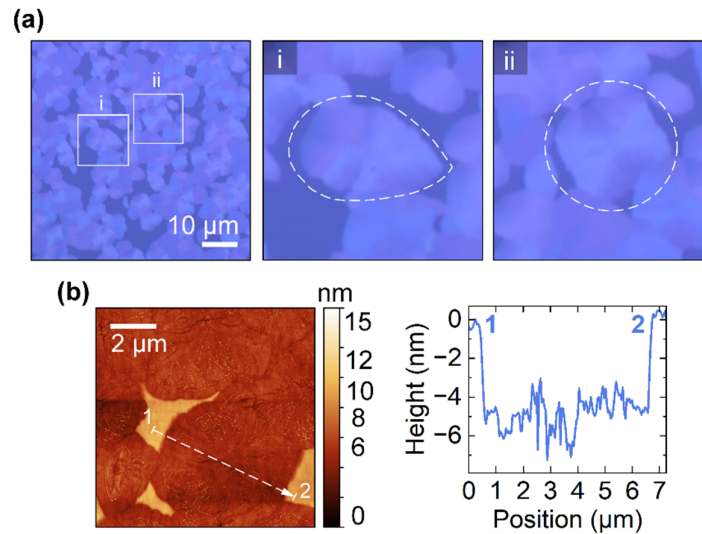


Figure S1. Sb_2Se_3 spherulites formed during growth at 150 $^{\circ}\text{C}$ on regrown GaAs. (a) Optical microscopy image of the as-grown film, showing spherulites occupy a partial fraction of the amorphous volume. Two variations of spherulite shapes are highlighted: (i) lenticular and (ii) spherical/radial form. (b) AFM scan of spherulite microstructure in the amorphous matrix. A height profile is shown for a selected line (labeled 1-2) through a spherulite. The elevated sections in the height profile represent the surrounding amorphous matrix.

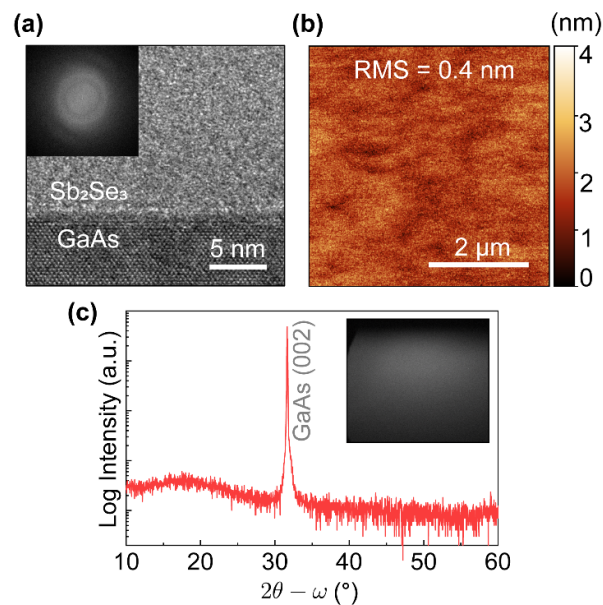


Figure S2. Amorphous Sb_2Se_3 phase grown below 150 $^\circ\text{C}$ on regrown GaAs. (a) (a) HR-TEM cross-sectional image and corresponding ring FFT of amorphous Sb_2Se_3 phase. (b) AFM of the amorphous film, showing a smooth surface of RMS roughness = 0.4 nm. (c) XRD out-of-plane 2θ - ω scan of the amorphous film showing no peaks arise from the film, only the substrate. The inset shows the hazy RHEED pattern observed during growth.

Partial spherulite crystallization of an amorphous matrix is observed for growth temperatures of 150 $^\circ\text{C}$. Optical microscopy and AFM images in Figure S1 highlight differences in optical appearance and topographic profiles between the spherulite domains and the amorphous matrix. Below 150 $^\circ\text{C}$, Sb_2Se_3 deposits as a majority amorphous phase. Multiple forms of structural characterization shown in Figure S2 (HR-TEM, AFM, XRD, and RHEED) confirm the disordered nature of the film at sub-150 $^\circ\text{C}$ growth temperatures.

C. Effect of Increasing Sb BEP

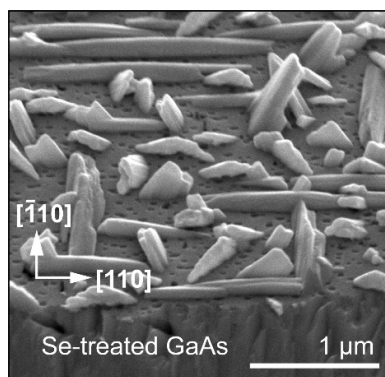


Figure S3. 45°-mounted SEM image of Sb_2Se_3 on Se-treated GaAs, grown with Sb and Se BEP of 2×10^{-7} Torr and 1×10^{-6} Torr, respectively. There is sparse coverage of Sb_2Se_3 across the substrate. Pitting of the GaAs substrate is also visible.

We find needle-like growth and very sparse coverage of Sb_2Se_3 crystals on the GaAs substrate achieved under a Sb and Se BEP of 2×10^{-7} Torr and 1×10^{-6} Torr, respectively (Figure S3). This film was prepared at 265 °C and a growth duration of 30 minutes, conditions that have produced coalesced films under the same Se BEP and lower Sb BEP of 5×10^{-8} Torr. (The growth rate is difficult to quantify here since we do not observe coalescence.) In Figure S3, most crystallites are observed to extend preferentially along the GaAs $[110]$ and $[\bar{1}10]$ directions, and a smaller fraction of crystallites grow at an inclined angle to the substrate. Too high a Sb BEP relative to Se clearly deteriorates the film morphology, as formation of the first and subsequent Sb_2Se_3 layers have been largely avoided.

D. Sb_2Se_3 Films on Rocksalt PbSe Template

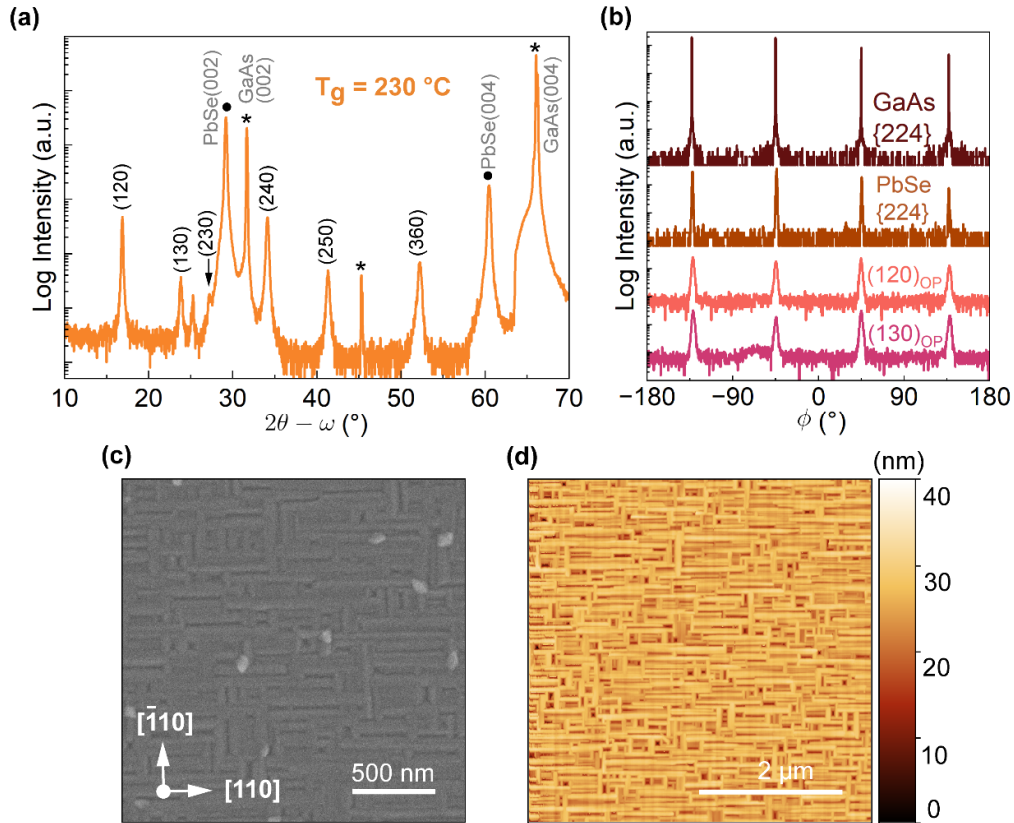


Figure S4. (a) XRD 2θ - ω scan showing (hk0)-oriented Sb_2Se_3 forms on a PbSe(001) template. (120) and (130)- Sb_2Se_3 are the dominant OP orientations. PbSe (001) peaks are denoted with a black circle, and GaAs peaks are denoted with an asterisk. The sharp peak near 45° is a scan artifact. (b) Phi scan of GaAs{224}, PbSe{224}, and the asymmetric (020)- Sb_2Se_3 plane for the two dominant (120) and (130)- Sb_2Se_3 OP orientations. The Sb_2Se_3 c-axis is aligned in-plane to the four cubic diagonals of PbSe. Film surface microstructure consists of rectangular features observed in (c) SEM and (d) AFM.

A PbSe nucleation and growth sequence adapted from Haidet *et al.*¹ was used to deposit 50 nm of high-quality epitaxial PbSe(001) on GaAs(001), and ~ 72 nm Sb_2Se_3 is grown thereafter on PbSe. The PbSe buffer thickness of 50 nm is greater than the critical thickness and therefore we assume the PbSe buffer layer is nearly relaxed to the bulk lattice constant of 6.12 \AA . We hypothesize that a PbSe template may present a more isotropic energy landscape along the $[110]$ and $[\bar{1}10]$ directions, creating a weaker bias for diffusion along one direction.

Sb_2Se_3 growth on PbSe indeed results in 90° -rotated grains aligned to the four cubic diagonals. XRD, SEM, and AFM characterization are shown in Figure S4. In Figure S4a and S4b, out-of-plane (OP) and phi scans indicate that the Sb_2Se_3 film is primarily (120)- and (130)-oriented OP, and that Sb_2Se_3 maintains the in-plane relationship $\text{Sb}_2\text{Se}_3 [001] \parallel \text{PbSe} \langle 110 \rangle$. Anti-parallel populations at $\phi = -135^\circ$ and 45° constitute the majority fraction in the film, and

the other two populations at $\varphi = -45^\circ$ and 135° show slightly weaker diffraction intensities in the phi scan. With the presence of 90° -rotated domains, neighboring grains impinge on one another at right angles to form the unique rectangular surface features apparent in Figures S4c and S4d. Rectangular features (instead of square) could arise from a deviation from ideal isotropy of the PbSe (001) template.

E. Effect of Decreasing Se BEP

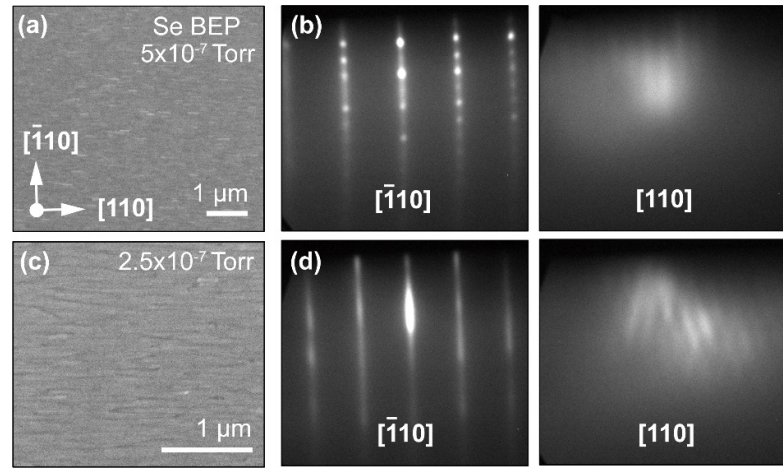


Figure S5. Sb_2Se_3 on regrown GaAs templates at $T_g = 200$ °C with Sb BEP = 5×10^{-8} Torr and variable Se BEP of 5×10^{-7} Torr and 2.5×10^{-7} Torr. (a) A Se/Sb BEP ratio = 10 yields parallel faceting and sub-micron “pill” structures as observed in SEM. (b) Sb_2Se_3 RHEED patterns along the GaAs $[110]$ and $[\bar{1}10]$ directions at 30 mins for the film shown in (a). The $[\bar{1}10]$ pattern is spotted along the main streaks and the $[110]$ streaks exhibit a higher periodicity but are noticeably weak. (c) A Se/Sb BEP ratio = 5 results in a slight misangle of the rod-like grains from the horizontal in-plane $[110]$ direction. (d) Sb_2Se_3 RHEED patterns for the film shown in (c). The $[\bar{1}10]$ pattern is streaky, and the $[\bar{1}10]$ pattern is complex with inclined intersecting streaks.

Two lower Se flux growth conditions were achieved by lowering the Se BEP (and keeping Sb BEP constant at 5×10^{-8} Torr). Surface microstructure and RHEED patterns are shown in Figure S5. The film morphology and crystallographic alignment are found to degrade with lower Se BEP. At $\text{Se} = 5 \times 10^{-7}$ Torr, grains still appear to primarily align to GaAs $[110]$; however, the $[\bar{1}10]$ RHEED pattern is spotty (Figure S5b). At the lowest explored Se BEP of 2.5×10^{-7} Torr, the RHEED pattern along GaAs $[110]$ has degraded from the usual observed vertical streaks (Figure S5d). The streaks are instead doubly inclined and intersecting one another. This film also adopts a “braided” surface appearance, where the ribbon-like grains exhibit a low angle in-plane tilt away from the horizontal GaAs $[110]$ directions (Figure S5c).

F. Repeatability of Epitaxial Films at $T_g = 200\text{ }^\circ\text{C}$

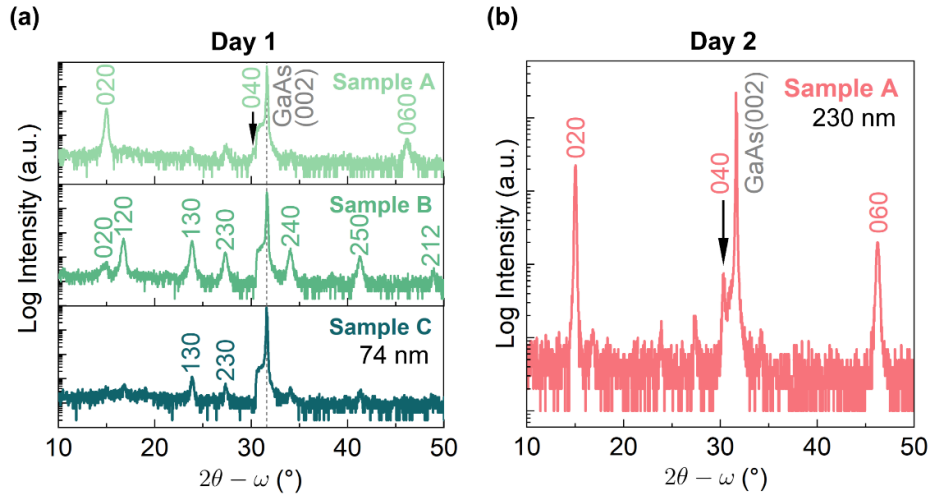


Figure S6. (a) Symmetric 2θ - ω scans of 74 nm films grown consecutively on Day 1 (Sample A, B, C) at $200\text{ }^\circ\text{C}$ on regrown GaAs, showing the (010) out-of-plane orientation is not consistently achieved after the first growth in the sequence. (b) 2θ - ω scan of first film (~ 230 nm) grown on Day 2 (Sample A), where the (010) orientation is again observed.

On the same day, we consecutively repeat three times the same $200\text{ }^\circ\text{C}$ synthesis procedure on regrown or homoepitaxial GaAs. We use Sb and Se BEPs of 5×10^{-8} Torr and 1×10^{-6} Torr, respectively, to achieve a growth rate of approximately 0.4 \AA/s . We find the (010) OP orientation of Sb_2Se_3 is no longer maintained after the first growth (Figure S6a). Due to the large Se beam pressure used, we speculate that the residual Se accumulated in the chamber over the duration of consecutive growths alters the substrate surface energy and therefore, the resulting stable crystalline orientations of Sb_2Se_3 . The desired (010) OP orientation is recovered and obtained on another day after the chamber has returned to baseline conditions (Figure S6b).

G. Mueller Matrix (MM) for As-Grown Crystalline Films

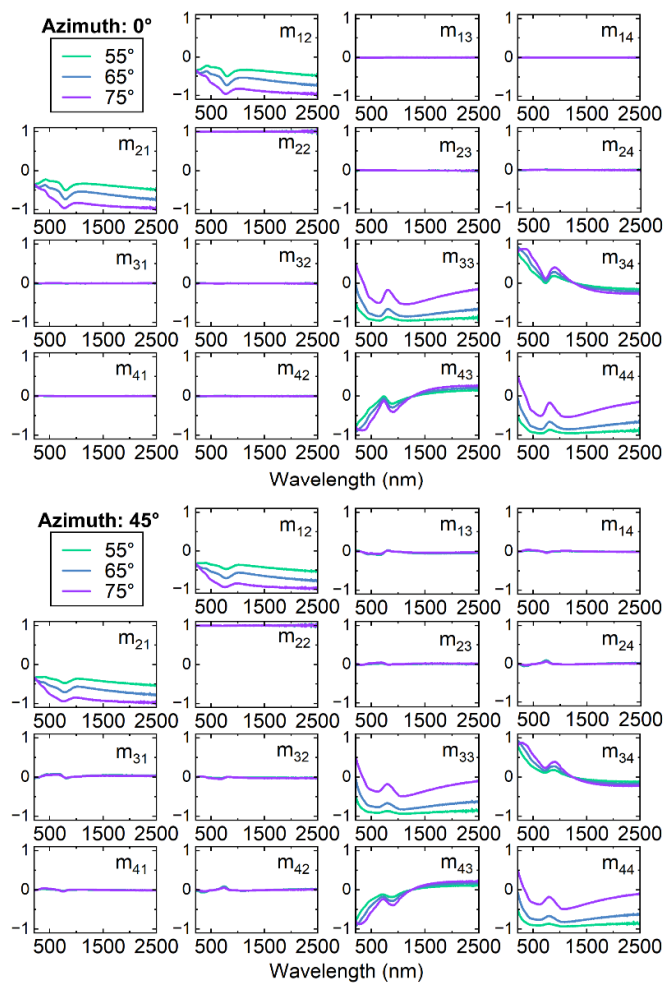


Figure S7. Mueller matrix for in-plane textured (hk0)-Sb₂Se₃ film across 210–2500 nm for 0° and 45° azimuthal rotation relative to the Sb₂Se₃ 1D axis.

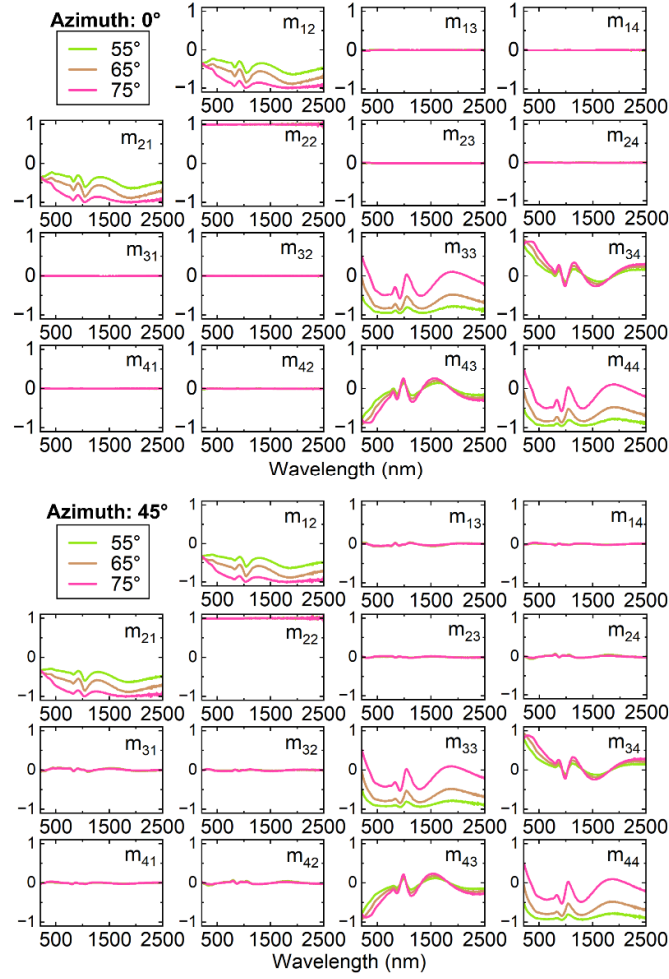


Figure S8. Mueller matrix for epitaxial (010)- Sb_2Se_3 film across 210–2500 nm for 0° and 45° azimuthal rotation relative to the Sb_2Se_3 1D axis.

Reflection-mode ellipsometry measurements were collected at three variable incidence angles of 55° , 65° , and 75° at approximately 0° , 45° , and 90° azimuthal sample rotations in the counter-clockwise direction relative to the Sb_2Se_3 1D axis direction. Data for 90° azimuthal orientation is not shown as it is represented well by measurements at 0° . At an azimuthal orientation of 45° , non-zero off diagonal blocks in the MM emerge (m_{13} , m_{14} , m_{23} , m_{24} and m_{31} , m_{32} , m_{41} , m_{42}), indicating optical anisotropy in the in-plane textured and (010)-epitaxial films (Figure S7 and S8).

References

1 B. B. Haidet, E. T. Hughes and K. Mukherjee, *Phys. Rev. Materials*, 2020, **4**, 033402.